IL NUOVO CIMENTO **41 C** (2018) 164
DOI 10.1393/ncc/i2018-18164-x

COLLOQUIA: IWM-EC 2018

Results and recent advances with the CHIMERA and FARCOS detectors

E. DE FILIPPO(1), L. ACOSTA(2)(1), L. AUDITORE(3), G. CARDELLA(1), A. CASTOLDI(4)(5), D. DELL'AQUILA(6), S. DE LUCA(3), F. FAVELA(1), B. GNOFFO(7)(1), C. GUAZZONI(4)(5), G. LANZALONE(8)(9), I. LOMBARDO(1), C. MAIOLINO(9), N.S. MARTORANA(7)(9), A. PAGANO(1), E.V. PAGANO(9), M. PAPA(1), T. PARSANI(4)(5), S. PIRRONE(1), G. POLITI(7)(1), F. PORTO(7)(9), L. QUATTROCCHI(1)(7), F. RIZZO(7)(9), P. RUSSOTTO(9), G. SACCÀ(1), A. TRIFIRÒ(3) and M. TRIMARCHI(3)

(1) *INFN, Sezione di Catania - Catania, Italy*
(2) *Instituto de Fisica, Universidad Nacional Autonoma de Mexico - Mexico City, Mexico*
(3) *Dipartimento di Scienze MITF, Università di Messina - Messina, Italy*
(4) *INFN, Sezione di Milano - Milano, Italy*
(5) *Dip. di Elettronica, Informazione e Bioingegneria, Politecnico di Milano - Milano, Italy*
(6) *INFN, Sezione di Napoli and Dip. di Fisica, Università di Napoli - Napoli, Italy*
(7) *Dip. Fisica e Astronomia, Università di Catania - Catania, Italy*
(8) *Università Kore - Enna, Italy*
(9) *INFN, Laboratori Nazionali del Sud - Catania, Italy*

received 3 December 2018

Summary. — The experimental activity with the CHIMERA 4π detector in the last two years is reviewed in the light of the most recent technical achievements of the device. In fact the CHIMERA detector capabilities are going to be extended with the implementation of a new digital front-end electronics and the coupling with the FARCOS ancillary correlator array. The device has reached a sufficient versatility in order to obtain results for different and specific data analysis with stable and radioactive heavy ion beams, *e.g.*, pygmy resonances, nuclear reactions of astrophysical interest, nuclear dynamics and study of the nuclear matter through the isospin degree of freedom. The obtained results and the expected future performances will be briefly discussed.

1. – Introduction

The strategy behind the recent scientific production involving the CHIMERA detector can be divided into two branches: the first one, prevalently by using up to now stable heavy-ions beams, devoted to the understanding, in the Fermi energy domain,

the processes responsible for particle productions in nuclear fragmentation, the reaction dynamics and the isospin degree of freedom. These studies of Nuclear Equation of State in asymmetric nuclear matter have been performed at lower density with respect to nuclear saturation density in the Fermi energy regime [1] and at high densities in the high incident energy domain [2].

Furthermore, the production of Radioactive Ion Beams (RIB) at LNS in the recent years has opened the use of the 4π detector CHIMERA to nuclear structure and clustering studies [3,4]. This requires to add to the charged particle identification techniques the capabilities to detect, with good efficiency, also γ-rays and/or neutrons and to develop new data analysis techniques in order, for example, to extract high-resolution angular distributions from kinematical coincidence measurements [5]. We remind that the capabilities of the CHIMERA detector for simultaneous mass and charge identification in the recent years were enhanced by integrating the Pulse Shape Detection method in the front-end electronics [6, 7] for the charged particles stopping in the first Silicon detection layer of the CHIMERA telescopes. More recently the CsI(Tl) detectors (the second detector layers of the CHIMERA telescopes) were exploited for γ-rays identification in the search of the isoscalar excitation of the Pygmy dipole resonance induced in ^{68}Ni inpinging on a Carbon target [8] and in the Hoyle-Gamma experiment at LNS [9]. In this latter experiment a ^{4}He (64 MeV) ions beam delivered by the Superconducting Cyclotron at INFN-LNS was used, bombarding a thin ^{12}C target. The goal of the experiment, related to the understanding the ^{12}C synthesis in the universe, is to measure the γ decay branching ratio of the 7.65 MeV Hoyle state of ^{12}C and the rare process of γ decay of higher excited levels (as the 3^-_1 state at 9.64 MeV) with respect to the 3α ^{12}C* decay [10]. The CHIMERA 4π setup is here exploited by measuring in coincidence α particles (by the ΔE-E method), ^{12}C recoil nucleus (by Time-of-Flight method) and γ-rays by pulse shape discrimination in CsI(Tl) scintillators.

High-energy and angular-resolution particle-particle correlation measurements are important tools in both nuclear structure and nuclear dynamics studies in order to characterize the time scale and shape of emission sources in the dynamical evolution of heavy-ion collisions. With this in mind, FARCOS, an ancillary and compact multi-detector with high angular granularity and energy resolution for the detection of light charged particles (LCP) and Intermediate Mass Fragments (IMF) has been designed [11-13] and its prototype has already been used under beam in many experiments. A generic and scalable electronic system, covering digitalization, signals readout, synchronization and triggering based on the GET electronics (General Electronics for TPCs) [14] has been adopted for FARCOS readout and for the CsI(Tl) readout of CHIMERA.

In the following, this paper will describe some selected aspects of the recent progress done by using both stable and Radioactive beams with the CHIMERA detector and the technical advances related to the adoption of a new front-end electronics for FARCOS and CHIMERA.

2. – Advances with RIBs beams

Figure 1 shows the experimental setup used in the PYGMY experiment [8]. Also if it refers to a particular experiment, it is a very emblematic example of a nowadays setup with CHIMERA + FARCOS devices and the use of in-flight radioactive beams. RIBs are produced by in-flight method [15] and delivered to the CHIMERA hall where the produced cocktail beam is analyzed event-by-event by the tagging system, constituted by a large surface Micro-Channel Plate (MCP) [16], giving the start of the Time-of-Flight

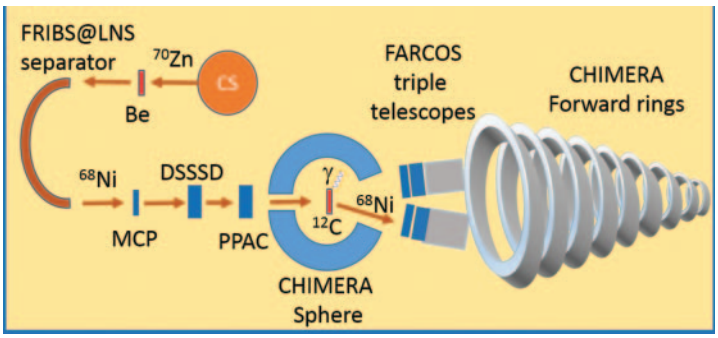

Fig. 1. – The experimental setup used in the ^{68}Ni+^{12}C experiment used for the search of the isoscalar excitation of the Pygmy Dipole Resonance in ^{68}Ni. In this experiment a 40 A MeV ^{70}Zn primary beam is used to produce the ^{68}Ni beam delivered by the FRIBs fragment separator.

(ToF) measurement. The stop of the ToF is delivered by a Double-Sided Silicon Strip Detector (DSSSD). The tagging system is completed by a position-sensitive Parallel Plate Avalanche Counter (PPAC), in order to get a beam trajectory measurement on the target. In this experiment four prototype telescopes of the FARCOS array are used, covering the angles between 2 and 7 degrees, in order to detect the isototopically identified ^{68}Ni ions. γ-rays are detected in the sphere as well neutrons. The latter limited to CHIMERA telescopes that are geometrically shielded by the FARCOS array. The experiment has shown evidence of the γ-ray decay of the pygmy resonance via an isoscalar probe [8]. A deeper analysis is currenty achieved [17] in order to look in the same experiment at the pygmy dipole resonance decay via neutron emission.

Results of particular relevance have been obtained by using the 55 A MeV $^{18}O^{7+}$ primary beam that, impinging on a 1.5 mm thick ^{9}Be target, produces a cocktail beam mainly populated by ions as ^{10}Be, ^{16}C, ^{13}B, etc., with intensities of the order 10^{4-5} pps. The produced beams are shown in fig. 2 as seen by the tagging DSSSD detector. In particular the cluster structure of ^{10}Be and ^{16}C have been studied via break-up reactions induced bombarding with these beams an hydrogenated (CH_2) target. The most relevant results have been shown in ref. [4] where, looking at the ^{4}He + ^{6}He break-up channel the ^{10}Be excitation energy E_x of the decaying nuclear states has been reconstructed. A new 6^+ state in ^{10}Be at 13.5 MeV was evidenced. A new experiment CLIR (Clustering in Light Ions Reactions) has been more recently done by using FARCOS for covering the most forward polar angles in place of the CHIMERA ones in order to increase granularity and energy resolution. The data analysis of the CLIR experiment is still in progress [18].

It is clear, from the few examples described above, how crucial is the project for the new FRAgment InFligh SEparator (FRAISE) at LNS, related to a general improvement and beams intensity upgrade (up to 2 kW) of the Superconducting Cyclotron at LNS [15] for the future activity of the CHIMERA detector and the associated devices. The production of RIBs from light to medium mass nuclei with increased intensity at Fermi energies has in fact a direct connection in order to progress in clustering phenomena, exotic break-up, transfer reactions and isospin physics for nuclear matter away from ground-state nuclei.

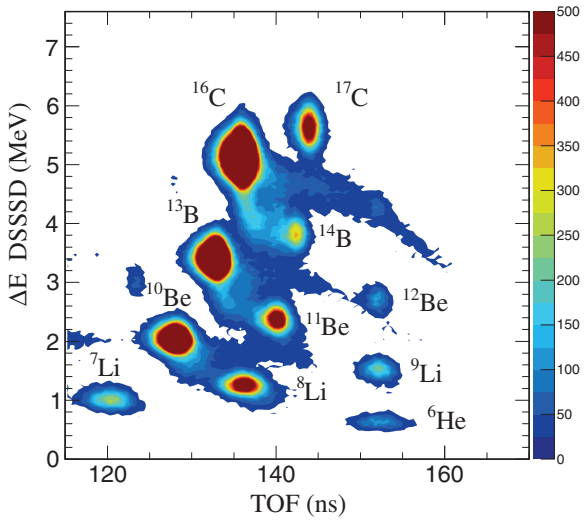

Fig. 2. – In the 32×32 silicon strips DSSSD tagging detector, correlation plot of energy loss ΔE *vs.* Time-of-Flight of cocktail beams induced by a primary ^{18}O beam on a beryllium target.

3. – Detection developments and technical progresses

The FARCOS array is constituted by 20 telescopes in the final project (complete realization is expected by the end of 2020). Each telescope is composed by three detection stages: the first ΔE is a 300 μm thick DSSSD silicon strip detector with 32×32 strips; the second is a DSSSD, 1500 μm thick with 32×32 strips; the final stage is constituted by 4 CsI(Tl) scintillators, each one 6 cm in length. A single FARCOS telescope has to handle around 196 readout channels taking into account a double amplification dynamics, limited to front strips. Thus the complete FARCOS array has around 4000 channels. For these reasons a generic and scalable electronic system, covering digitalization, signals readout, synchronization and triggering based on the GET electronics (General Electronics for TPCs) has been adopted and extended to the readout of the whole 1192 CsI(Tl) detectors of the CHIMERA array. The GET electronics is described in detail in ref. [14] and references therein.

It is based on the integrated circuit AGET chip, originally designed for Time Projection Chambers (TPCs) and active targets devices and has been adapted for CsI(Tl) scintillators of CHIMERA and Silicon strip detectors and CsI(Tl) of FARCOS array. In fact, the pre-amplification stage embedded in the AGET chip is by-passed in order to use the existing CHIMERA pre-amplifiers operating under vacuum. A new CMOS front-end in the Silicons and CsI(Tl) on ASIC boards for the FARCOS array has been designed [19, 20]. Signals coming from the pre-amplifiers are interfaced to the GET system through a Dual Gain Module. This last is a multichannel digitally programmable gain amplifier, two ways splitter and level adapter, interfaced to the AGET inputs. In this way the large dynamic range of more than 10^3 required by CHIMERA and FARCOS devices can be achieved. Figure 3(a) shows the model of the geometrical setup we are preparing in order to use 10 telescopes of the FARCOS array in the "CHIFAR" experiment expected to run at beginning of 2019. This ring-like configuration will be mounted between the last ring of CHIMERA and the beginning of the sphere at around 30°. Note

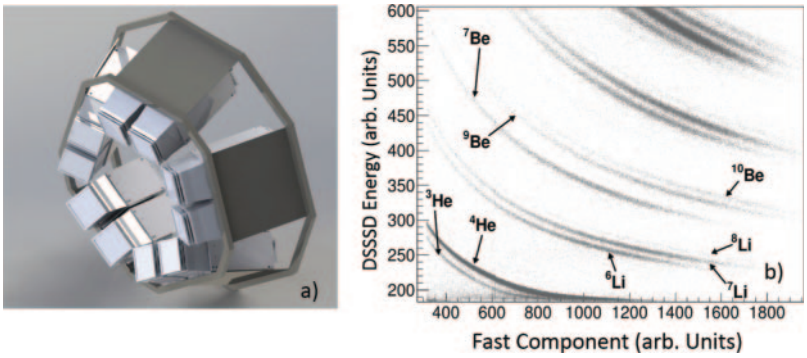

Fig. 3. – (a) Model of the mechanical setup of 10 modules of FARCOS array designed for the CHIFAR experiment (see text). (b) ΔE-E (DSSSD 1500 μm - CsI) bidimensional light particles identification plot in a FARCOS module in the CLIR experiment (adapted from ref. [18]). In this experiment data readout was done with standard electronic front-end and analog data acquisition (DAQ).

that each wall of the telescope acts as a basis for the internal motherboards housing the front-end electronics and managing the signals and bias voltages from DSSSDs, to which are connected by means of kapton cables [13]. Figure 3(b) shows an example of a ΔE-E (DSSSD 1500 μm - CsI) matrix collected by a FARCOS prototype with standard electronic front-end and analog readout during the CLIR experiment [18]. The good isotopic identification obtained for light ions is clearly seen.

A part of the CHIMERA 4π detector, limited to CsI(Tl) detectors, will use the GET front-end electronics as well the FARCOS telescopes. On the other hand, the current electronic and readout front-end based on VME analog readout for silicon detectors are expected to continue to be used. The coupling of the two data acquisition under a common supervisor and a common trigger configuration is described in some detail in [21]. Figure 4(a) shows schematically the data flow from the front-end electronics

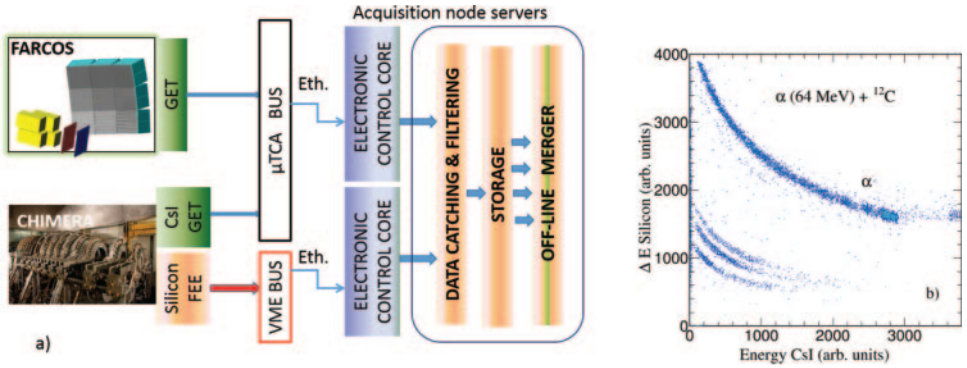

Fig. 4. – (a) Schematic view of the hybrid Analog-VME Digital-GET data acquisitions coupling. (b) ΔE-E bidimensional plot for a telescope of ring 10 in the CHIMERA sphere in the reaction α+^{12}C at 64 MeV (Hoyle-Gamma experiment) obtained after data merging of Silicon readout (VME DAQ) and CsI readout (GET digital DAQ). In the Hoyle-Gamma experiment the FARCOS array was not present.

(FEE) to the data storage and off-line merging. The Hoyle-Gamma experiment was the first one in which the GET digital electronics was used for the readout of the all CsI(Tl) scintillators of the CHIMERA backward part (the Sphere, $30° < \theta < 176°$). Dual Gain modules were used to split all CsI signals in two different gains in particular in order to improve the signal to noise ratio for the low energy γ-rays. Figure 4(b) shows the ΔE energy loss in silicon *vs.* residual energy in CsI for a telescope at $\theta = 34°$. In this bidimensional plot the ΔE is obtained by the analog front-end and VME DAQ while the x-axis (residual energy) is obtained by signal analysis of the pulse height distribution of the relative CsI(Tl) channel in the GET digital electronic.

A further important development for the near future is the capability to add the neutron detection to the list of available observables. In fact this is a critical point in particular when working with RIB facilities and neutron rich nuclei. We started a research project aimed to develop the prototype of a plastic scintillator array in order to detect neutrons in coincidence with light charged particles or IMFs to be coupled or integrated to other devices. Results of a study on EJ-299-33 scintillators with radioactive sources and by using heavy-ion reactions have been recently presented [22,23]. A specific contribution to this argument can be found here [24].

4. – Advances in reaction dynamics at Fermi energies

When studying the nuclear dynamics of heavy-ion collisions at Fermi energies in a broad range of projectile-target combinations one is faced with a remarkable range of values in the time-scales of different mechanisms from early out-of-equilibrium emission (few fm/c) up to statistical decay or fission (hundreds or thousands of fm/c). Understanding the production times of fragments and the mechanisms responsible for particle and fragments emission is a key issue, in particular related to the link with the isospin degree of freedom and nuclear Equation of State [1]. The most recent results of experiments with the CHIMERA device are the investigation on Isospin equilibration by using the time derivative of total dipole signal in the reaction ^{48}Ca+^{27}Al at 40 A MeV [25] and the study of competition between statistical and dynamical emission in projectile-like break-up as a function of the N/Z isospin of the entrance channel. In this section we expose this last topic showing the recent results obtained from data analysis of the InKiIsSy experiment (Inverse Kinematic Isobaric System) on ^{124}Xe+^{64}Zn and ^{64}Ni collisions at 35 A MeV.

We studied the IMF production probability and emission mechanism in the projectile-like fission or break-up by using, as main observable, the angle $\cos(\theta_{prox})$ between the center-of-mass velocity of the kinematical reconstructed PLF* with respect to the relative velocity of the PLF* break-up fragments in order to estimate the probability between statistical and dynamical IMFs emission as a function of the IMF atomic number. Note that this angle, often referred as $\cos(\alpha)$, has been used also as a "chronometer" in order to study the rotation of the binary fissioning system [26] as a function of the N/Z of the break-up fragments [27, 28]. The most important points of this analysis are: i) the selections of events in which the IMF multiplicity M_{IMF} is strictly equal to one; ii) the rejection of events in which IMFs originate from TLFs fragmentation or decay; iii) the dynamical component is obtained by subtracting from the total $\cos(\theta_{prox})$ distribution, the portion of angular distribution that is symmetric around $\cos(\theta_{prox}) = 0$. Details of the data analysis can be found in ref. [29]. Results have been compared with previous studied reactions ^{124,112}Sn + ^{64,58}Ni at the same incident energy [30]. In this latter work, it was shown that binary statistical break-up was equally probable for the two Sn + Ni

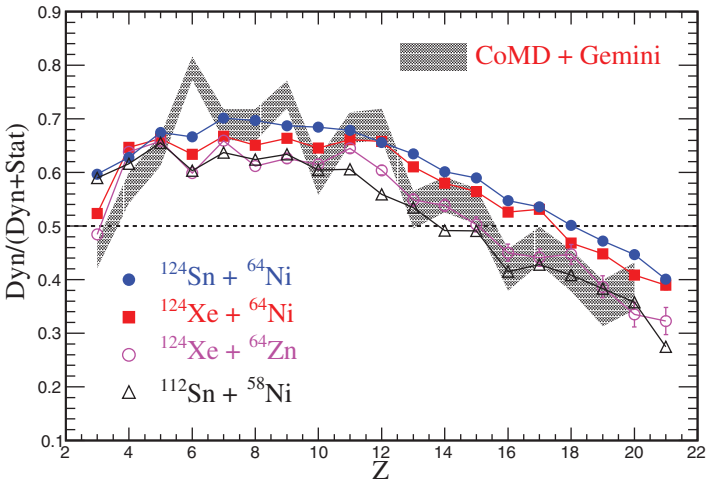

Fig. 5. – Ratio of the dynamical component *vs.* the total (statistical + dynamical) as a function of the IMF atomic number Z for three isobaric systems plus the ^{112}Sn+^{58}Ni reaction (empty triangles). The hashed cyan area indicates results of a CoMD + GEMINI simulation (see text) for the ^{124}Xe+^{64}Ni system.

neutron rich/neutron poor systems. On the contrary the dynamical break-up is favored for neutron rich system and it depends upon the IMFs atomic number. By using isobaric systems, any size (mass) effect is ruled out and the results can only be attributed to the different N/Z ratios of the entrance channel.

Figure 5 highlights the main result: it shows the ratio of the dynamical component with respect to the dynamical+statistical one as a function of the IMFs atomic number for the three isobaric systems ^{124}Xe + ^{64}Ni, ^{124}Xe + ^{64}Zn and ^{124}Sn + ^{64}Ni. For comparison also the non-isobaric ^{112}Sn + ^{58}Ni reaction is reported. Thus, the IMFs dynamical emission probability (for $Z_{IMF} > 7$) is enhanced by the increase of the N/Z, in particular it increases just changing the N/Z of the target (from ^{64}Zn to ^{64}Ni). In ref. [29] it is further quantitatively shown, in comparing the four studied systems, that the dynamical emission probability is twice more sensitive to an increase of the target N/Z content with respect to the projectile one.

These results provide an important test for microscopic transport models. In fig. 5 we present as a dashed area a comparison of the experimental data for the reaction ^{124}Xe + ^{64}Ni with a preliminary simulation in the frame of the constrained molecular dynamics, CoMD-III code [31]. Within this model, the ^{124}Xe + ^{64}Ni reaction at 35 A MeV is simulated up to 600 fm/c. After this point, the secondary decay of fragments is followed by using the GEMINI code. The data are analysed as the experimental ones, and the fraction of dynamical emitted IMFs is calculated as a function of the IMFs atomic number. Data were filtered by the detector geometry. The comparison between data and calculation (that have to be extended to the other reactions studied) seems very promising. It is interesting to note that the CoMD model gives also the possibility to vary the isospin-dependent part of the interaction in order to provide different parametrizations of the symmetry energy component of the EOS [25,32,33]. This will be a very interesting aspect to be further studied in detail as well as the investigation, in the simulation code, of dynamics and shape instabilities leading to the projectile-like binary break-up as a function of the time evolution of the reaction and isospin content of the entrance channel.

In 2019 we shall extend these studies at a lower beam incident energy in the transition energy region from Coulomb to Fermi energies, around 20 A MeV, with stable beams ("CHIFAR" experiment), by using the CHIMERA device coupled with 10 modules of the FARCOS correlator (with the setup described in fig. 3a).

5. – Advances in nuclear symmetry energies at high densities

The equation of state in neutron-rich matter, expressed in the parabolic law approximation [34] as $\mathrm{EOS}(\rho,\beta) = E_0(\rho)+E_{sym}(\rho)\beta^2+\ldots$, where E_0 is the energy in symmetric matter, $\beta = (\rho_n - \rho_p)/\rho$ is the isospin asymmetry as a function of neutrons, protons and nuclear matter density respectively and $E_{sym}(\rho)$ is the nuclear "symmetry energy", provides fundamental understanding in nuclear physics, astrophysics phenomena and the physics of dense objects like neutron stars [35]. It is widely recognized that $E_{sym}(\rho)$ at supra-saturation densities is badly constrained from experimental point of view due to lack of data while theoretical calculations in many-body theories give controversial results for $E_{sym}(\rho)$ behavior predictions at high densities. The ASYEOS experiment at GSI has been specifically conceived in order to constrain the symmetry energy behavior of the EOS at supra-saturation densities by measuring direct and elliptic flows of neutrons and light charged particles in the reactions $^{197}\mathrm{Au} + {}^{197}\mathrm{Au}$ at 400 A MeV [2]. The basic idea behind this experiment is that the ratio of the neutron-proton elliptic flow v_2 can be used to probe the high-density component of the symmetry energy because it reflects the squeeze-out (emission perpendicular to the reaction plane) of nuclear matter from the compressed high-density region interaction zone [36]. The density dependence of $E_{sym}(\rho)$ can be expanded in a Taylor series with respect to the density:

$$E_{sym}(\rho) = S_0 + \frac{L}{3}\left(\frac{\rho-\rho_0}{\rho_0}\right) + \frac{K_{sym}}{18}\left(\frac{\rho-\rho_0}{\rho_0}\right)^2 + \ldots,$$

where L and K_{sym} are, respectively, the slope and curvature parameters of the symmetry energy at ρ_0 and S_0 is the value of symmetry energy at ρ_0.

In order to measure the direct and elliptic flows of neutron and charged particles emitted at mid-rapidity, the LAND detector [37] was used. Flow parameters, for neutrons and light charged particles, are constructed looking at their azimuthal distributions with respect to the reference reaction plane. The latter was determined event-by-event by using four rings of the CHIMERA array and Aladin Time-of-Flight device. The obtained results, described in ref. [2], can be highlighted in three main points: i) the ratio of neutrons and charged particle elliptic flow is a robust observable for probing the the EOS at high densities; ii) the constrain, obtained by comparison with the UrQMD transport model, corresponds to the value of $L = 72 \pm 13$ MeV with a considerable smaller uncertainty with respect to the previous FOPI data results [36]; iii) a systematic analysis was done in order to calculate the density range really explored in the reaction as a function of the observables used and for different transport models. In the ASYEOS experiment this value has a range ρ/ρ_0 between 0.8 and 1.6 as resulting by calculations with the Tübingen QMD model [2, 38].

Recent new data from astrophysical observations on neutron stars and gravitational waves [39, 40] call for new experiments exploring the symmetry energy in the region $1.5 < \rho/\rho_0 < 3$ only available by heavy-ion collisions at relativistic energies. This can be done by using improved detection devices and new available radioactive beams at FAIR where systems with larger asymmetries could be studied. A first point that can

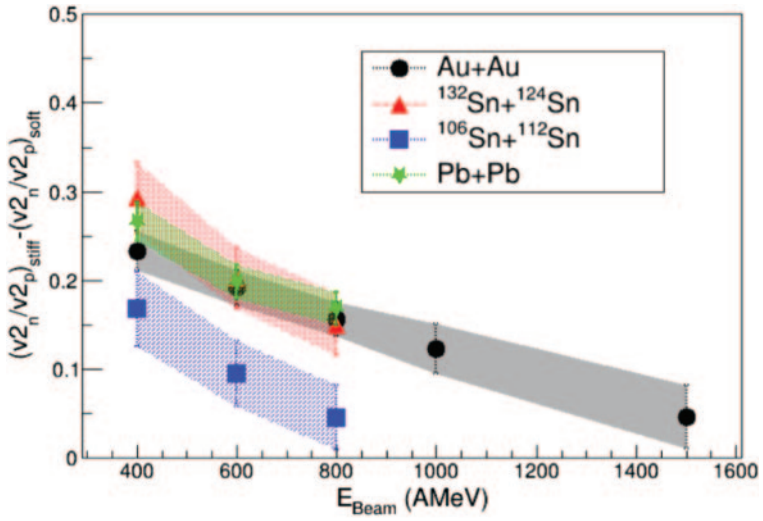

Fig. 6. – UrQMD simulations showing the model sensitivity to the difference of the neutron/proton elliptic flow v_2 ratio $(v_2^n/v_2^p)_{stiff} - (v_2^n/v_2^p)_{soft}$ as a function of the incident beam energies for the indicated heavy-ion reactions. Here stiff and soft refers to values of $\gamma = 1.5$ and $\gamma = 0.5$ parametrizzation of the potential component of the symmetry energy.

be addressed is to explore the sensitivity of the neutron/protons flow ratio observable at higher densities increasing the beam incident energies in the region between 400 A MeV and 1500 A MeV. Figure 6 shows results of UrQMD calculations in which the sensitivity of the elliptic flow ratio of neutrons with respect to protons to the symmetry energy parametrization, reported as a function of beam incident energies. Sensitivity of the elliptic flow is expressed as the difference $(v_2^n/v_2^p)_{stiff} - (v_2^n/v_2^p)_{soft}$. For Au + Au collisions this difference decreases only slightly up to 1000 A MeV incident energy allowing discrimination between stiff and soft choice of the symmetry energy parameters. Therefore future experiments can significantly explore higher-density regions by using the elliptic flow ratio of neutrons and protons as a main observable. Indeed sensitivity to higher densities is increased if the neutron *vs.* protons flow is used as main observable. Because in this new experiment a good identification of neutrons and isotopically separated hydrogen with high resolution is a fundamental task, it is envisaged to use the NeuLAND detector, that is part of the R^3B project [41] for FAIR at GSI, as a main device for a new ASYEOS-II experiment [42].

6. – Conclusions

An overview of the recent activity with the CHIMERA and FARCOS devices in the recent years has been presented. In particular, it was shown that the steady improvements in the detection techniques and front-end electronics, related to the new experimental and physical needs and to the increasing interest in the use of radioactive beams at LNS, has opened the use of the 4π detector to nuclear structure and clustering studies. A big effort has been dedicated, in this contest, to the construction of the new FARCOS array, designed for multi-particle correlations and "femtoscopy" studies. Particular relevance has been given to the recent findings of the isoscalar excitation above the neutron emission threshold of the Pygmy Dipole Resonance in ^{68}Ni by using a radioactive beam and

the circumstantial evidence of Isospin effects in dynamical production of Intermediate Mass Fragments. This latter experiment done by using stable cyclotron beams. Finally, we have shown a summary of results of ASYEOS experiment and the high interest and effort done in order to propose a new experiment constraining the symmetry energy at 2–3 ρ_0 in the GSI-FAIR facility.

* * *

Results presented in this paper have been obtained within CHIMERA collaborations for CLIR, PYGMY, INKIISSY, Hoyle-Gamma experiments, respectively. ASYEOS results are obtained within the ASYEOS collaboration.

REFERENCES

[1] De Filippo E. and Pagano A., *Eur. Phys. J. A*, **50** (2014) 32.
[2] Russotto P. *et al.*, *Phys. Rev. C*, **94** (2016) 034608.
[3] Cardella G. *et al.*, *Nucl. Instrum. Methods Phys. Res. A*, **799** (2015) 64.
[4] Dell'Aquila D. *et al.*, *Phys. Rev. C*, **93** (2016) 024611.
[5] Cardella G. *et al.*, *Nucl. Instrum. Methods Phys. Res. A*, **715** (2013) 56.
[6] Alderighi M. *et al.*, *IEEE Trans. Nucl. Sci.*, **52** (2005) 1624.
[7] Alderighi M. *et al.*, *IEEE Trans. Nucl. Sci.*, **53** (2006) 279.
[8] Martorana N. S. *et al.*, *Phys. Lett. B*, **782** (2018) 112.
[9] Cardella G. *et al.*, *Measurement of the γ-decay branching ratio of the Hoyle and first excited 3^- levels of ^{12}C*, experiment proposal PAC-LNS (2016).
[10] Tsumura M. *et al.*, *J. Phys.: Conf. Ser.*, **569** (2014) 012051.
[11] FARCOS Technical Design Report 2015, available on-line at: `https://drive.google.com/file/d/0B5CgGWz8LpO0c3pGTWdOcDBoWFE`.
[12] Pagano E. V. *et al.*, *EPJ Web of Conferences*, **117** (2016) 10008.
[13] Acosta L. *et al.*, *J. Phys.: Conf. Ser.*, **730** (2016) 012001.
[14] Pollacco E. C. *et al.*, *Nucl. Instrum. Methods Phys. Res. A*, **887** (2018) 81.
[15] Russotto P. *et al.*, *J. Phys.: Conf. Ser.*, **1014** (2018) 012016.
[16] Lombardo I. *et al.*, *Nucl. Phys. B*, **215** (2011) 272.
[17] Martorana N. S., these proceedings.
[18] Dell'Aquila D. *et al.*, *Acta Phys. Pol. B*, **48** (2017) 499.
[19] Castoldi A., Guazzoni C. and Parsani T., *IEEE Trans. Nucl. Sci.*, **64** (2017) 2678.
[20] Guazzoni C., these proceedings.
[21] De Filippo E. *et al.*, *J. Phys.: Conf. Ser.*, **1014** (2018) 012003.
[22] Pagano E. V. *et al.*, *Nucl. Instrum. Methods A*, **889** (2018) 83.
[23] Pagano E. V. *et al.*, *Nucl. Instrum. Methods A*, **905** (2018) 47.
[24] Pagano E. V., these proceedings.
[25] Papa M. *et al.*, *Phys. Rev. C*, **91** (2015) 041601.
[26] Jedele A. *et al.*, *Phys. Rev. Lett.*, **118** (2017) 062501.
[27] De Filippo E. *et al.*, *Phys. Rev. C*, **86** (2012) 014610.
[28] Hudan S. *et al.*, *Phys. Rev. C*, **86** (2012) 021603.
[29] Russotto P. *et al.*, arXiv:1803.03046.
[30] Russotto P. *et al.*, *Phys. Rev. C*, **91** (2015) 014610.
[31] Papa M., *Phys. Rev. C*, **87** (2013) 014001.
[32] Cardella G. *et al.*, *Phys. Rev. C*, **85** (2012) 064609.
[33] Stiefel K. *et al.*, *Phys. Rev. C*, **90** (2014) 061605.
[34] Bombaci I. and Lombardo U., *Phys. Rev. C*, **44** (1991) 1892.
[35] Baldo M. and Burgio G. F., *Prog. Part. Nucl. Phys.*, **91** (2016) 203.

[36] Russotto P. *et al.*, *Phys. Lett. B*, **697** (2011) 471.
[37] Blaich T. *et al.*, *Nucl. Instrum. Methods*, **314** (1992) 136.
[38] Cozma M. D., *Phys. Lett. B*, **700** (2011) 139.
[39] Fattoyev F. J., Piekarewicz J. and Horowitz C. J., *Phys. Rev. Lett.*, **120** (2018) 172702.
[40] Zhang N.-B. and Li B.-A., arXiv:1807.07698 (2018).
[41] `http://www.gsi.de/r3b`.
[42] Russotto P. *et al.*, *Determination of symmetry energy at supra-saturation densities: A feasibility study*, S464 GPAC LoI.